Available online at www.sciencedirect.com
ScienceDirect
Journal of Nuclear Materials 363–365 (2007) 728–732
journal of nuclear materials
www.elsevier.com/locate/jnucmat

Examination of the velocity time-delay-estimation technique

J.H. Yu *, C. Holland, G.R. Tynan, G. Antar, Z. Yan

University of California, San Diego, 9500 Gilman Dr., MC 0417, La Jolla, CA 92093, USA

Abstract

The one-dimensional time-delay-estimation (TDE) velocity technique infers the velocity of plasma fluctuations using cross-correlations between two spatially separated signals, and here this technique is evaluated using experimental results and numerical simulations. Probe arrays and a fast-framing imaging camera are used to measure the azimuthal fluctuation propagation speed in a cylindrical magnetized plasma device. The time-averaged TDE velocity field obtained in this way is found to be approximately 30% larger than Mach probe measurements of the plasma fluid velocity, suggesting that the TDE method infers the plasma $E \times B$ velocity and presumably a diamagnetic flow. The TDE technique is also applied to turbulent simulation data with known velocity fields. The results show that for the TDE parameters chosen here, the TDE technique can be used to infer the large-scale, slowly varying velocity, but that small scale or turbulent velocity fields cannot be reliably inferred.

PACS: 52.30.−q; 52.35.Ra; 52.35.Kt

Keywords: Cross-field transport; Edge plasma; Fluctuations and turbulence; Plasma flow

1. Introduction

Measurements of both the time-averaged and turbulent plasma velocity fields are desirable to validate theories and simulations of edge plasma turbulence, edge plasma flows, material migration, and plasma surface interactions. Several schemes for inferring the plasma velocity field from time-resolved imaging diagnostics have recently been proposed [1–3]. The simplest of these schemes is based on the cross-correlation analysis of two spatially separated fluctuation measurements, and we denote this technique as the velocity time-delay-estimation (TDE).

The TDE method has a rich history in neutral fluids [4]. In recent work the TDE method is applied to density fluctuation measurements obtained with beam emission spectroscopy [5], showing the existence of geodesic acoustic modes [6] (GAMs), which are finite frequency zonal flows [7] and are believed to be a major player in edge turbulence in DIII-D and other machines such as ASDEX Upgrade, JFT-2M, and the CHS stellarator. The TDE technique is being pursued as a way to infer the turbulent velocity associated with turbulent fluxes at locations inside the separatrix [5,8]. Caution should be used, however, when applying the results of the TDE algorithm to quantify the actual advection of

* Corresponding author. Fax: +1 858 534 7716.
E-mail address: jyu@ferp.ucsd.edu (J.H. Yu).

0022-3115/$ - see front matter © 2007 Elsevier B.V. All rights reserved.
doi:10.1016/j.jnucmat.2007.01.253

particles (which is due only to guiding center drifts such as $E \times B$ flow). The fluctuations generally cannot be treated as passive tracers in a background advecting flow, because diamagnetic effects can generate a phase velocity relative to the guiding center velocity [9].

In this paper, we focus on steady flows in the experiments, and compare the 1D TDE scheme applied to probes and imaging data. Both the probes and the fast-framing imaging yield similar TDE velocity profiles, opening the possibility of using images to infer the velocity field in regions where probes cannot be used. The TDE measurement is then compared to Mach probe measurements of the ion fluid velocity. We use simulations to further understand how the TDE technique relates to $E \times B$ drifts and diamagnetic effects.

2. TDE method

Fluctuations (density, potential, or image intensity) are sampled at rate $1/\Delta t$, and the time lag τ_p is calculated between the two spatially separated signals based on the peak of the cross correlation $R_{\Delta x}(\tau) = \frac{1}{T}\int_{t-T/2}^{t+T/2} \mathrm{d}t' n(x,t') n(x+\Delta x, t'+\tau)$, where n is the measured signal and T is the duration over which each cross correlation is calculated. From the peak time lag and known separation distance Δx, the TDE velocity is calculated as $V_{\mathrm{TDE}} = \Delta x/\tau_p$. By moving the time window T and repeating the calculation, an ensemble of different realizations is used in calculating V_{TDE}, thus reducing the error. Denoting the total number of time windows as N, the TDE velocity can be obtained by finding the mean velocity from N time windows, allowing a measure of the statistical variation in V_{TDE}. Alternatively, the N correlation functions from all time windows can be averaged, and the mean velocity found from the peak of the average correlation function. We have tested both methods and they yield similar results; in the data presented here, we use the method that allows error bars to be calculated from the statistical variation.

The range of velocities that the TDE method can reliably infer is limited by the fact that the signals are discretely sampled over a finite time window. If we denote the length of the time window under consideration as T, then there is a maximum lag that can be inferred, $\tau_{\max} = T/2$, which in turn specifies a *minimum* velocity magnitude $V_{\min} = \Delta x/\tau_{\max}$ that can be inferred. Discrete sampling implies that there is a *maximum* velocity magnitude that can be inferred, $V_{\max} = \Delta x/\Delta t$, such that fluctuations do not move a distance Δx in a time faster than Δt. Note that interpolation can be used to reduce the size of Δt significantly below the sampling period. In addition, the timescale τ_{decor} for the turbulence to decorrelate must be longer than the time window T so that the flow is approximately steady within T, because the TDE method relies on the Taylor frozen-flow hypothesis. Therefore, the range of inferable velocity magnitudes is bounded, with the range given by

$$2\frac{\Delta x}{\tau_{\mathrm{decor}}} < 2\frac{\Delta x}{T} < |V| < \frac{\Delta x}{\Delta t}. \quad (1)$$

In Ref. [3], the TDE method was applied to test signals with known velocity fields in the presence of noise, showing that the TDE method reliably infers the mean velocity with magnitude greater than or equal to $0.2\ \Delta x/\Delta t$ with signal to noise ratios larger than 10, and reliably infers time-dependent flows if the flow varies sufficiently slowly ($f < 2/T$).

3. Experimental set-up and results

The experiments are performed with the Controlled Shear De-correlation Experiment (CSDX) plasma device, which uses an azimuthally symmetric half-wavelength helicon antenna operating at 13.56 MHz with 1500 W of power (less than 20 W is reflected), with an Argon gas pressure of 3.0 mTorr. The plasma source radius is approximately 4.5 cm and is connected to a downstream cylindrical chamber of 10 cm radius and approximately 3 m length which is immersed in a solenoidal magnetic field of 1 kG (directed from the downstream end of the chamber toward the source). The field lines terminate on insulating surfaces in the plasma source and on the downstream end the field lines terminate on an insulating vacuum window, through which an axial view of the plasma column is recorded with a fast-framing camera. All of the probe data shown here are obtained at a distance 75 cm downstream from the exit plane of the plasma source, sampled at 1 MHz with azimuthal probe separation $\Delta x = 0.5$ cm. At 1 kG, the ion cyclotron frequency for Argon $f_{\mathrm{ci}} = \Omega_{\mathrm{ci}}/2\pi = 38$ kHz, the sound speed $C_s = \sqrt{T_e/M_i} = 2.7 \times 10^5$ cm/s (using $T_e = 3.0$ eV), and ion-sound gyroradius $\rho_s = C_s/\Omega_{\mathrm{ci}} = 1.1$ cm; the density scale length (in the region of strongest gradient) $L_n = (\mathrm{d}\ln n_0/\mathrm{d}x)^{-1} \approx 3$ cm. A more detailed description of the

plasma source and fluctuation characteristics can be found in the literature [10–13].

A four tip Mach probe is used to measure the plasma flow velocity, in both the parallel and perpendicular directions with respect to the axial magnetic field. The measurement is based on taking the ratio R_M of ion saturation currents from two 180° opposed probes. By rotating the Mach probe, R_M is measured as a function of the angle θ between the line connecting opposing probes and **B**. Following recent work by Shikama et al. [14], we then fit the data with a function of the form $R_M = \exp\left[K \sin \Delta\alpha/\Delta\alpha\left(M_{par}\cos\theta + M_{perp}\sin\theta\right)\right]$, where $\Delta\alpha$ is the acceptance angle of each probe tip, M_{par} and M_{perp} are used as fitting parameters, and we use Hutchinson's model of ion collection [15] with $K = 1.34$. Mach probe results have been previously checked against spectroscopic Doppler shift measurements [16], and against PIC simulations [17].

Fig. 1 shows the TDE velocity obtained from probes and fast-framing imaging, compared with the azimuthal fluid velocity measured with the Mach probe. Here, the Mach probe velocity $v_M = C_s(r)M_{perp}$ includes radial variation of C_s due to $T_e(r)$. Applying the TDE algorithm to the probe data yields a velocity profile shown by the red points. Images of the plasma viewed along an axial line-of-sight are obtained with a Phantom v.7.1 fast-framing camera, using a frame rate of 67 kHz and spatial resolution of 64×64 pixels. We apply the TDE technique to 1500 frames of broadband emission intensity recorded by two pixels that image two azimuthally-separated locations in the plasma. The results demonstrate that the TDE technique applied

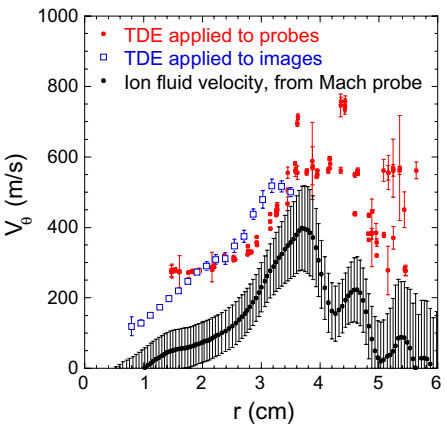

Fig. 1. The velocity measured using the two-point correlation TDE technique from both probes and fast-framing imaging, compared to the ion fluid velocity measured with a Mach probe.

to imaging data agrees with the TDE velocity obtained from probes. We also observe that the TDE velocity is approximately 30% larger than the ion fluid velocity measured by the Mach probe. The results suggest that the fluctuations are advected by the plasma $E \times B$ flow and have an inherent phase velocity v_ϕ, which is presumably given by the dominant drift mode plasma-frame phase velocity driven by diamagnetic effects.

4. Simulation and results

We can quantify the significance of the diamagnetic contribution to the TDE velocity using results from drift turbulence simulations with known advecting velocities and known pressure gradients, that is, with known $E \times B$ and drift wave phase velocities. Using a modified Hasagawa–Wakatani model [18] to describe a simple drift-wave system, we have applied the TDE technique to fluctuations that naturally result from the turbulent simulation. The equations used in the simulation are given by

$$\frac{dn}{dt} + \tilde{V}_x \frac{dn_0}{dx} + \omega_{||}(n - \phi) = D\nabla_\perp^2 n, \tag{2}$$

$$\frac{d\nabla_\perp^2 \phi}{dt} + \omega_{||}(n - \phi) = \mu\nabla_\perp^4 \phi, \tag{3}$$

where the tilde denotes fluctuating quantities, the mixing-length normalized fluctuating density and potential are given by $n = (L_n/\rho_s)(\tilde{n}/n_0)$ and $\phi = (L_n/\rho_s)(e\tilde{\phi}/T_e)$, μ is the normalized ion viscosity, the time scales have been normalized by C_s/L_n, and the spatial scales have been normalized by ρ_s. The 'adiabatic parameter' $\omega_{||} \equiv k_{||}^2 v_{th_e}^2/\upsilon_e$ quantifies the degree to which the Boltzmann relation $n_e = n_0 \exp(-e\phi_{tot}/k_B T_e)$ is maintained via parallel electron dynamics (where v_{th_e} is the electron thermal speed and υ_e is the electron collision frequency). Here, the total derivative includes advection by the turbulent velocity $\tilde{V} = -\nabla\phi \times \hat{z}$, and advection by an externally imposed mean flow V^0:

$$\frac{df}{dt} = \frac{\partial f}{\partial t} + \tilde{V} \cdot \vec{\nabla} f + V^0 \frac{\partial f}{\partial y}, \tag{4}$$

where the modification to the original Hasegawa–Wakatani model is the addition of the second advection term $V^0\partial_y f$. This slowly varying flow is given by $V_y^0(x,t) = U^0 \sin(k_x x)[1 + 0.5\cos(\omega_V t)]$, which is a shear flow in the y direction with steady and slowly oscillating components. This velocity field is intended to represent the advection of small-scale turbulent density fluctuations due to GAMs (the slowly

varying component of V_y^0) and other large-scale shear flows which are important components of drift-wave turbulence in tokamaks [7]. The scale of the externally imposed shear flow is large, and is equal to the radial box size $L_x = L_y = 64\ \rho_s$ such that $k_x = 2\pi/L_x$; and the flow frequency is $\omega_V = 2\pi C_s/10L_n$.

The simulations are performed in a two-dimensional periodic box with 256 points used in each direction. The external flow parameter U_0 is set to 2.5, giving a strength of V_y^0 significantly stronger than the turbulent flow, but not so strong as to completely overpower the turbulence (RMS $V_y^0 = \frac{3}{2\sqrt{2}} U_0 \sin(k_x x) \approx 2.7 \sin(k_x x)$, RMS $\tilde{V}_y = 0.72$). A snapshot of the turbulent density field is given in Fig. 2(a). The TDE technique was applied to the density field at all radial and poloidal positions using an interpolation factor of 10 and poloidal separation of 1 ρ_s (well within the poloidal correlation length which is 5–6 ρ_s for all fluctuating quantities).

Snapshots of the inferred and actual poloidal velocity field are presented in Fig. 2(b) and (c). In general, the macroscopic (large-scale, slowly varying) components of the velocity are well inferred in the regions where there is a significant mean velocity, but the technique does not accurately infer the small-scale components of the flow, or the flow as a whole in regions of small mean flow.

To further analyze the TDE method, the inferred and actual mean poloidal flows are shown in Fig. 3(a). The black curve represents the time and flux-averaged total poloidal flow V_{sim} from the

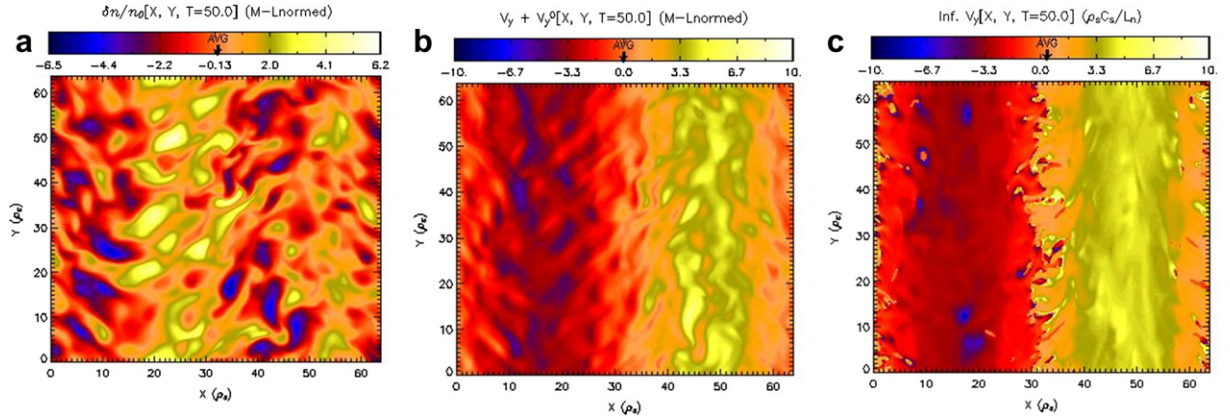

Fig. 2. Snapshots from the simulation of (a) the density fluctuations, (b) the actual velocity field and (c) the TDE-inferred velocity field. The large-scale features are captured by the TDE method; however, the small scale structures are lost.

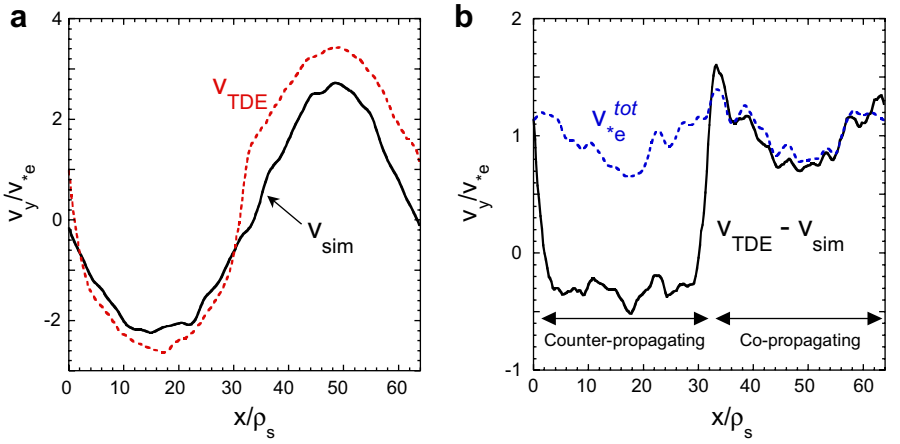

Fig. 3. (a) Comparison of the time and flux-averaged poloidal velocity from the simulation (solid black) with the TDE-inferred velocity (dashed red). (b) The difference between $V_{TDE} - V_{sim}$ is surprisingly close to the total diamagnetic velocity in the region where the externally imposed flow propagates in the same direction as the electron diamagnetic velocity. The counter-propagating region shows quite different behavior. (For interpretation of color in Fig. 3, the reader is referred to the web version of this article.)

simulation, and the red dashed curve is the TDE-measured velocity V_{TDE}. There is general agreement, but a small offset is seen which is dominant in the region $x > 32\,\rho_s$. Fig. 3(b) shows that in this region, where the mean flow is propagating in the electron diamagnetic direction, the offset between V_{TDE} and V_{sim} is given by the 'total' diamagnetic velocity V_{*e}^{tot}. Thus, for the co-propagating case, the TDE method infers the sum of the $E \times B$ velocity and the total diamagnetic velocity, defined as

$$V_{*e}^{\mathrm{tot}} \equiv -\frac{\rho_s C_s}{\langle n_{\mathrm{tot}} \rangle} \frac{\mathrm{d}\langle n_{\mathrm{tot}} \rangle}{\mathrm{d}x} \approx -\frac{\rho_s C_s}{n_0} \left(\frac{\mathrm{d}n_0}{\mathrm{d}x} + \frac{\mathrm{d}\langle \tilde{n} \rangle}{\mathrm{d}x} \right) = V_{*e} \left(1 - \frac{\mathrm{d}\langle n \rangle}{\mathrm{d}x} \right), \quad (5)$$

where $\mathrm{d}\langle n \rangle / \mathrm{d}x$ represents the normalized fluctuating density gradient, and the brackets refer to an average over flux surface (i.e. average over y) and time. The total diamagnetic velocity consists of the standard diamagnetic velocity $V_{*e} \equiv -\rho_{sCs}/L_n$, plus a term that results from the turbulent fluctuations modifying the background density gradient. In regions where the mean flow is opposed to the electron diamagnetic direction ($x < 32\,\rho_s$), the agreement between V_{*e}^{tot} and $V_{\mathrm{TDE}} - V_{\mathrm{sim}}$ is poor; however, the fluctuations are in phase with each other. We currently do not have an understanding for the discrepancy in the counter-propagating region, which will be the subject of future work.

5. Discussion and conclusions

The TDE technique applied to fluctuations measured with probes and applied to emission data from fast-framing imaging yield velocity profiles that are in good agreement. Based on the experiments and simulations presented here, we believe that the TDE-measured fluctuation phase velocity in the lab frame is given by the $E \times B$ drift velocity plus any plasma-frame phase velocity (caused by diamagnetic effects). Thus, there are limitations in using the TDE technique to study particle transport, because the diamagnetic velocity component that is measured by the TDE method does not contribute to particle advection, which is caused by guiding center drifts. In addition, particle fluxes are driven by turbulent velocity fields, and correlation-based algorithms such as TDE fail to infer rapidly varying ($f > 2/T$) flows with velocities smaller than $2\Delta x/T$. The TDE technique can, however, be used to infer large-scale, slowly varying velocities, such as the equilibrium and slowly varying $E \times B$ flow within a flux surface in the scrape-off-layer of tokamaks. In the case of diamagnetic flow directed opposite to the $E \times B$ flow, the nonlinear dynamics are different from the co-propagating case, and further work is needed to understand the TDE results in the counter-propagating regions.

Acknowledgements

This research was performed under US Department of Energy (DOE) grants DE-FG02-04ER54773 and DE-FG02-04ER54734. CH performed this research under appointment to the Fusion Energy Postdoctoral Research Program administered by the Oak Ridge Institute for Science and Education under contract number DE-AC05-00OR22750 between the US DOE and Oak Ridge Associated Universities.

References

[1] G.R. McKee, R.J. Fonck, D.K. Gupta, D.J. Schlossberg, M.W. Shafer, Rev. Sci. Instrum. 75 (2004) 3490.
[2] J.L. Terry, S.J. Zweben, O. Grulke, M.J. Greenwald, B. LaBombard, J. Nucl. Mater. 337–339 (2005) 322.
[3] C. Holland, G.R. Tynan, G.R. McKee, R.J. Fonck, Rev. Sci. Instrum. 75 (2004) 4278.
[4] Y.T. Chan, J.M.F. Riley, J.B. Plant, IEEE Trans. Acoust. Speech. ASSP-29 (1981) 577.
[5] G.R. McKee, R.J. Fonck, M. Jakubowski, K.H. Burrell, K. Hallatschek, R.A. Moyer, D.L. Rudakov, W. Nevins, G.D. Porter, P. Schoch, X. Xu, Phys. Plasmas 10 (2003) 1712.
[6] K. Hallatschek, D. Biskamp, Phys. Rev. Lett. 86 (2001) 1223.
[7] P.H. Diamond, S.-I. Itoh, K. Itoh, T.S. Hahm, Plasma Phys. Control. Fus. 47 (2005) R35.
[8] M. Jakubowski, R.J. Fonck, G.R. McKee, Phys. Rev. Lett. 89 (2002) 265003-1/4.
[9] D.W. Horton, Rev. Mod. Phys. 71 (1999) 735.
[10] G.R. Tynan, A.D. Bailey III, G.A. Campbell, R. Charatan, A. de Chambrier, G. Gibson, D.J. Hemker, K. Jones, A. Kuthi, C. Lee, T. Shoji, M. Wilcoxson, J. Vac. Sci. Technol – A 15 (1997) 2885.
[11] J. George, Experimental Study of Linear Resistive Drift Waves in a Cylindrical Helicon Plasma Device, MS thesis, Department of Mechanical and Aerospace Engineering, University of California, San Diego, 2002.
[12] G.R. Tynan, M.J. Burin, C. Holland, G. Antar, N. Crocker, P.H. Diamond, Phys. Plasmas 11 (2004) 5195.
[13] M. Burin, G. Antar, N. Crocker, G.R. Tynan, Phys. Plasmas 12 (2005) 052320.
[14] T. Shikama, S. Kado, A. Okamoto, S. Kajita, S. Tanaka, Phys. Plasmas 12 (2005) 044504.
[15] I.H. Hutchinson, Plasma Phys. Control. Fus. 47 (2005) 71.
[16] T. Shikama, S. Kado, A. Okamoto, S. Kajita, S. Tanaka, J. Nucl. Mater. 337–339 (2005) 1077.
[17] J.P. Gunn et al., Phys. Plasmas 8 (2001) 1995.
[18] A. Hasegawa, M. Wakatani, Phys. Rev. Lett. 50 (1983) 682.